International Journal of Power Electronics and Drive System (IJPEDS)
Vol. 4, No. 1, March 2014 pp. 81~90
ISSN: 2088-8694

Total Harmonic Distortion Analysis of a Four Switch 3-Phase Inverter Fed Speed Sensorless Control of IM Drives

ZMS El-Barbary*, HZ Azazi, MK Metwally **
* Departement of Electrical Engineering, Kaferelsheikh University, Egypt
** Departement of Electrical Engineering, Menoufiya University, Egypt

Article Info

Article history:

Received Nov 2, 2013
Revised Feb 4, 2014
Accepted Feb 21, 2014

Keyword:

Four switch inverter
Induction motor
Sensorless speed control
Six switch inverter
Total harmonic distortion
Digital signal processor

ABSTRACT

This paper investigates the performance of a Model reference adaptive system (MRAS) based cost-effective drive system of an induction motor (IM) for low-cost applications - high performance industrial drive systems. In this paper, the MRAS is used as a speed estimator and the motor is fed from a four-switch three-phase (FSTP) inverter instead of a conventional six-switch three-phase (SSTP) inverter. This configuration reduces the cost of the inverter, the switching losses, and the complexity of the control algorithms and interface circuits, the proposed control approach reduces the computation for real-time implementation. The robustness of the proposed MRAS-based FSTP inverter fed IM drive is verified by Experimental results at different operating conditions using digital signal processor (DSP1103) for a 1.1 Kw motor. A performance comparison of the proposed FSTP inverter fed IM drive with a conventional SSTP inverter system is also made in terms of speed response and total harmonic distortion (THD) of the stator current. The proposed FSTP inverter fed IM drive is found quite acceptable considering its performance, cost reduction and other advantages features.

Corresponding Author:

ZMS El-Barbary
Departement of Electrical Engineering,
Kaferelsheikh University,
Kaferelsheikh, Egypt,
Email : z_elbarbary@yahoo.com

1. INTRODUCTION

The induction motors are called the workhorse of the motion industry because they are most widely used motors for appliances, industrial control, and automation. They are robust, reliable, simple, cheap and available in all power ratings. The squirrel cage types of induction motors are very popular in variable-speed drives. When AC power is supplied to an induction motor at certain specifications, it runs at its rated speed. However, many applications need variable speed operations. Due to the progress in the field of semiconductor field i.e. power electronics and Integrated circuits enables the application of induction motors for high-performance drives. These power electronics not only control the motor's speed, but can improve the motor's dynamic and steady state characteristics. In addition, this improves the energy savings and reduces noise generation of the motor. A standard three-phase voltage source inverter utilizes three legs (six-switch three-phase voltage source inverter or SSTPI), with a pair of complementary power switches per phase. A reduced switch voltage source inverter (four switch three-phase voltage source inverter or FSTPI) uses only two legs, with four switches. The Several papers report on FSTPI structure, Most of the reported works on 4-switch, 3-phase (FSTP) inverter for machine drives did not consider the closed loop vector control scheme, which is essential for high performance drives. Induction motor drives have been thoroughly studied in the past few decades and many vector control strategies have been proposed, ranging from low cost to high performance applications. Traditionally, 6-switch, 3-phase (SSTP) inverters hive been widely utilized for variable speed IM drives. This involves the losses of the six switches as well as the complexity of the control algorithms and interface circuits to generate six PWM logic signals [1].

In the past, researchers mainly concentrated on the development of the efficient control algorithms for high performance variable speed IM drives However, the cost, simplicity and flexibility of the overall drive system which become some of the most important factors did not get that much attention to the researchers. That's why, despite tremendous research in this area most of the developed control system failed to attract the industry.

Usually, high performance motor drives used in robotics, rolling mills, machine tools, etc. require fast and accurate response, quick recovery of speed from any disturbances and insensitivity to parameter variations. The dynamic behavior of an AC motor can be significantly improved using vector control theory where motor variables are transformed into an orthogonal set of d-q axes such that speed and torque can be controlled separately. This gives the IM machine the highly desirable dynamic performance capabilities of a separately excited DC machine, while retaining the general advantages of the ac over DC motors [2, 3].

In this paper, a cost effective FSTP inverter fed sensorless IM drive is developed. The four switches makes the inverter less cost, less switching losses, less chances of destroying the switches due to lesser interaction among switches, less complexity of control algorithms and interface circuits as compared to the conventional SSTP inverter, the proposed control approach reduces the computation for real time implementations. Furthermore, the use of speed sensorless for induction motor drives besides being reduce bulky and increase the robustness, it reduce additional electronics, extra wiring, extra space. And reduce extra cost to the drive system, Speed sensor, also, implies and careful mounting which detracts from the inherent robustness of the drive.

The proposed sensorless control method verifies the validity of an MRAS-based FSTP inverter fed IM drive system for cost reduction and other advantages such as reduced switching losses, reduced number of interface circuits to supply logic signals for the switches, easier control algorithms to generate logic signals. Thus, the main issue of this paper is to analysis a cost effective, simple and efficient high performance IM drive.

The performance of a closed-loop vector control scheme of the proposed FSTP inverter fed IM speed sensorless drive is implemented using digital signal processing DSP1103 interfaced with the MATLAB/SIMULINK software. A comparison of the proposed FSTP inverter fed IM drive with a conventional SSTP inverter system is also made experimentally in term of total harmonic distortion (THD) of the stator current and speed response. The proposed inverter fed IM drive is found good considering its cost reduction and other advantageous.

2. DRIVE SYSTEM

The control scheme of low cost induction motor drive consists of the modeling of the IM, inverter, sensorless control and the controller, which are discussed in the following subsections:

A. Four Switch Three-Phase Inverter

This inverter is configured with four switches $Q_{1,}$ Q2, Q3 and Q4, respectively, as shown in figure 1. Two output phases are taken from the inverter legs directly where the third output is taken from the midpoint of the two capacitors. The inverter converts the DC-voltage to a balanced three-phase output with adjustable voltage and frequency.

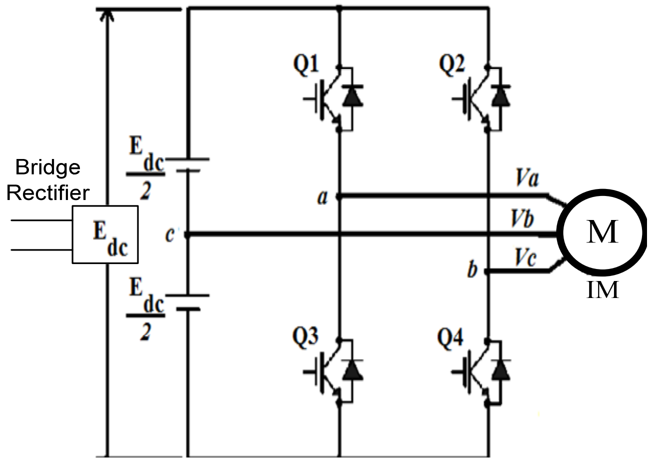

Figure 1. Four switch three- phase inverter with IM

In the analysis, the inverter switches are considered as ideal power switches and it is assumed that the conduction state of the power switches is associated with binary variables Q1 to Q4. Therefore, a binary "1" will indicate a closed state, while "0" will indicate the open state. Pairs Q1 to Q3 and Q2 to Q4 are complementary and as a sequence: (Q1 = 1-Q3, Q4 = 1-Q2). Two control possibilities exist to control the four-switch bridge inverter, i.e., two- level current control to force the two controlled phases currents to sinusoidal, or using PWM to control the voltages applied to the three-phase quasi- sinusoidally. The two-level current control of the four-switch bridge inverter used to control the load current by forcing it to follow a reference one. This is achieved by the switching action of the inverter to keep the current within the hysteresis band. The load currents are sensed and compared with respective command currents using two independent hysteresis comparators. The output signals of the comparators are used to activate the inverter power switches.

This controller is simple and provides excellent dynamic performance. The modulated phases voltages of four switch inverter are introduced as a function of switching logic NA, NA1, NB and NB1 of power switches by the following relations [4].

$$V_a = .\frac{E_{dc}}{3}(4NA + 2.NB - 1). \tag{1}$$

$$V_b = .\frac{E_{dc}}{3}(-2NA + 4.NB - 1). \tag{2}$$

$$V_c = .\frac{E_{dc}}{3}(-2NA - 2.NB + 2). \tag{3}$$

In matrix form,

$$\begin{bmatrix} V_a \\ V_b \\ V_c \end{bmatrix} = \frac{E_{dc}}{3}\begin{bmatrix} 4 & 2 & -1 \\ -2 & 4 & -1 \\ -2 & -2 & 2 \end{bmatrix}\begin{bmatrix} NA \\ NB \\ 1 \end{bmatrix} \tag{4}$$

Where, NA1 and NB1 are complementary of NA and NB, Also, it will be assumed that a stiff voltage is available across the two dc-link capacitors

B. Induction Motor Model

Squirrel-cage induction motor is represented in its d-q dynamic model. This model represented in synchronous reference frame is expressed as follows;

$$\begin{bmatrix} V_{qse}^{e} \\ V_{dse}^{e} \\ 0 \\ 0 \end{bmatrix} = \begin{bmatrix} R_s + pL_\sigma & \omega_e L_\sigma & p\frac{L_m}{L_r} & \omega_e \frac{L_m}{L_r} \\ -\omega_e L_\sigma & R_s + pL_\sigma & -\omega_e \frac{L_m}{L_r} & p\frac{L_m}{L_r} \\ -R_r L_m & 0 & R_r + pL_\sigma & (\omega_e - \omega_r) L_m \\ 0 & -R_r L_m & -(\omega_e - \omega_r) L_m & R_r + pL_\sigma \end{bmatrix} \begin{bmatrix} I_{qs}^{e} \\ I_{ds}^{e} \\ \lambda_{qr}^{e} \\ \lambda_{dr}^{e} \end{bmatrix} \quad (5)$$

The electromechanical equation is also given by;

$$T_e - T_L = J\frac{d\omega_r}{dt} + B\omega_r \quad (6)$$

Where, the electromagnetic torque is expressed as;

$$T_e = \frac{3}{2}\frac{p}{2}.\frac{L_m}{L_r}(I_{qs}^{e}\lambda_{dr}^{e} - I_{ds}^{e}\lambda_{qr}^{e}) \quad (7)$$

C. Spees Estimator Based on Mras

Model Reference Adaptive Systems (MRAS) techniques applied in order to estimate rotor speed. This technique is based on the comparison between the outputs of two estimators. The outputs of two estimators may be (the rotor flux, back emf, or motor reactive power). The estimator that does not involve the quantity to be estimated (The rotor speed ω_r) is considered as the induction motor voltage model. This model considered to be the reference model (RM). The other model is the current model, derived from the rotor equation, this model considered to be the adjustable model (AM). The error between the estimated quantities by the two models is used to drive a suitable adaptation mechanism which generates the estimated rotor speed [5].

In this paper, the observer depends on the MRAS technique. The speed observer is based on stator current and rotor flux as state variables [9]. The speed estimating procedures from the stator current error are as follows:

First, from the induction motor equation the stator current is represented as:

$$\begin{aligned} i_{ds} &= \frac{1}{Lm}\left[\lambda_{dr} + \omega_r T_r \lambda_{qr} + T_r p\lambda_{dr}\right] \\ i_{qs} &= \frac{1}{Lm}\left[\lambda_{qr} - \omega_r T_r \lambda_{qr} + T_r p\lambda_{qr}\right] \end{aligned} \quad (8)$$

Using Equation (8), and estimated instead of measured speed, the stator current is estimated as

$$\begin{aligned} \hat{i}_{ds} &= \frac{1}{Lm}\left[\lambda_{dr} + \hat{\omega}_r T_r \lambda_{qr} + T_r p\lambda_{dr}\right] \\ \hat{i}_{qs} &= \frac{1}{Lm}\left[\lambda_{qr} - \hat{\omega}_r T_r \lambda_{qr} + T_r p\lambda_{qr}\right] \end{aligned} \quad (9)$$

Form the relationship between the real stator current and the estimated stator current, the difference in the stator current is obtained as

$$\begin{aligned} i_{ds} - \hat{i}_{ds} &= \frac{T_r}{Lm}\lambda_{qr}\left[\omega_r - \hat{\omega}_r\right] \\ \hat{i}_{qs} - i_{qs} &= \frac{T_r}{Lm}\lambda_{dr}\left[\omega_r - \hat{\omega}_r\right] \end{aligned} \quad (10)$$

In Equation (10), the difference of stator current is sinusoidal value because it is the function of rotor flux. Multiplying by the rotor flux and adding them together;

$$\begin{aligned}(i_{ds} - \hat{i}_{ds})\lambda_{qr} &= \frac{T_r}{Lm}\lambda^2_{qr}\left[\omega_r - \hat{\omega}_r\right] \\ (\hat{i}_{qs} - i_{qs})\lambda_{dr} &= \frac{T_r}{Lm}\lambda^2_{dr}\left[\omega_r - \hat{\omega}_r\right]\end{aligned} \tag{11}$$

By summing the above two equations.

$$(i_{ds} - \hat{i}_{ds})\lambda_{qr} + (\hat{i}_{qs} - i_{qs})\lambda_{dr} = \frac{T_r}{Lm}(\lambda^2_{qr} + \lambda^2_{dr})\left[\omega_r - \hat{\omega}_r\right] \tag{12}$$

Hence, the error of the rotor speed is obtained as follows:

$$\begin{aligned}&\omega_r - \hat{\omega}_r = [(i_{ds} - \hat{i}_{ds})\lambda_{qr} - (i_{qs} - \hat{i}_{qs})\lambda_{dr}]/K \\ &Where \qquad K = \frac{T_r}{Lm}(\lambda^2_{qr} + \lambda^2_{dr})\end{aligned} \tag{13}$$

The right hand term seems as the term of speed calculation from adaptive observer, so the speed can be calculated from the following equation [8]:

$$\begin{aligned}\hat{\omega}_r = \frac{1}{K}[(&K_p(i_{ds} - \hat{i}_{ds})\lambda_{qr} - (i_{qs} - \hat{i}_{qs})\lambda_{dr}) + \\ &(K_I \int (i_{ds} - \hat{i}_{ds})\lambda_{qr} - (i_{qs} - \hat{i}_{qs})\lambda_{dr})]\end{aligned} \tag{14}$$

Figure 2 shows The MRAS system.

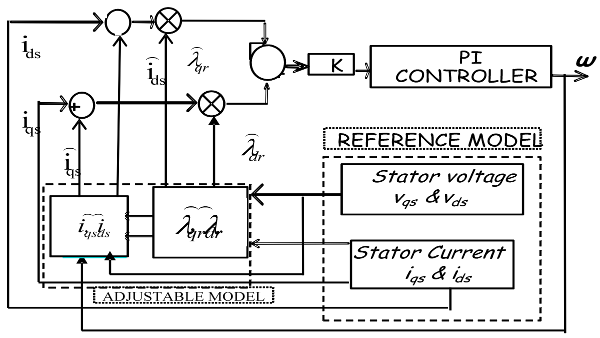

Figure 2. Block Diagram for the Speed Estimation Procedure

C. Overall System Contrller

As shown in Figure 3. It incorporates the speed controller which receives the error signal between the preset speed and the actual observed speed of the motor shaft and then generates the torque command (T_e^*) through a proportional integral (PI) speed controller. This torque command produces the quadrature current command I_{qs}^{*e} in the synchronous reference frame (SYRF). The direct current I_{ds}^{*e} is sets by the rotor flux level λ_{dr}^{*e}. This flux level is calculated according to the method described in [6]. The two current commands are then transformed to the stationary reference frame (STRF) with the aid of the calculated command angle (θ_e^*). This command angle is calculated in such away that aligns the direct-axis of SYRF with the rotor flux axis. The two stator current commands, I_{qs}^{*e} and I_{ds}^{*e} in the SYRF are then transformed to STRF and then transformed to three phase references current i_{ar},i_{br} and i_{cr}. Only, two currents reference i_{ar} and i_{br} required for the hysteresis current controller that generates the switching function for the pulse width modulated voltage source inverter.

3. EXPERMENTAL RESULTS

To verify the validity of the proposed system, an induction motor vector control system was constructed. Figure 4 shows a block diagram of the experimental system, which was composed of a DSP board DSP 1103 [10], Two phases currents and voltages I_a , I_b and V_a,V_b are sensed by Hall-effect current and voltage sensors. These signals are fed to the DSP through the signal conditioning circuit. Also the speed of the rotor is sensed by 2048 PPR incremental encoder for detecting the motor speed and fed to the encoder interface on the DSP board. The control algorithm is executed by 'simulink' [11], and downloaded to the board through host computer. The outputs of the board are logic signals, which are fed to the three-phase inverter through driver and isolation circuits. The performance of the conventional six switch inverter based sensorless IM drive system and proposed system is compared at different operating conditions with the proposed MRAS-based FSTP inverter fed IM experimentally. The response due to a step change in the speed command is used to evaluate the performance in terms of steady state errors and stability both at no load and full load conditions. Figure 5.a shows the estimate and measured speed response with a command speed of 90 rad/sec at no load at t=0.9 second, the speed reference has been changed to 120 rad/sec. It can be seen that the rotor speed is accelerated smoothly to follow its reference value with nearly zero steady state error. Figure 5.b shows the motor phase current and its reference whereas Figure 5.c shows the motor three phase current . The motor current increase with increasing speed and return back to its normal value. These results show a good correlation between the estimated speed signal and its corresponding measured as well as reference speed signals. The total harmonic distortion (THD) of i_a is found 27.0386% as shown in Figure 5(d)

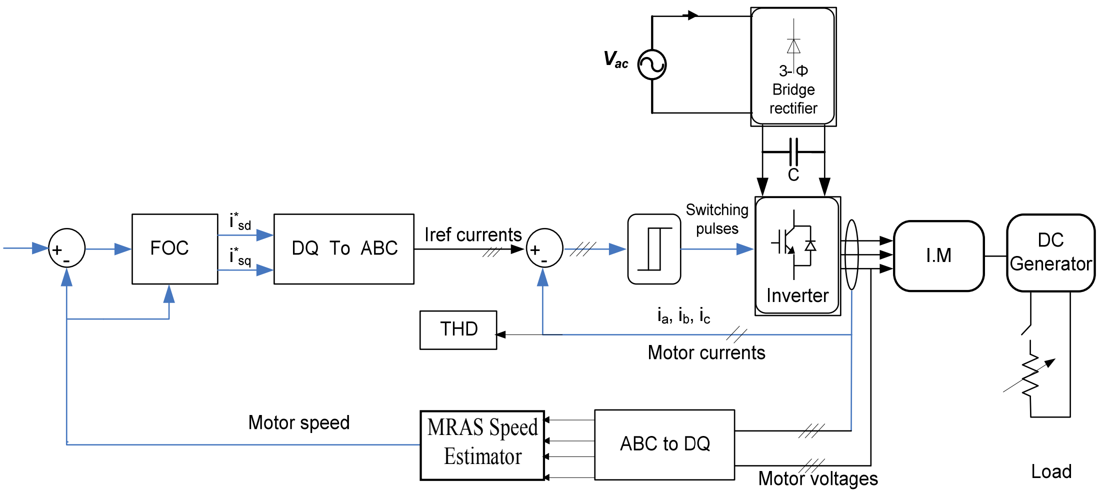

Figure 3. Block diagram for a vector-controlled induction motor based on speed estimation

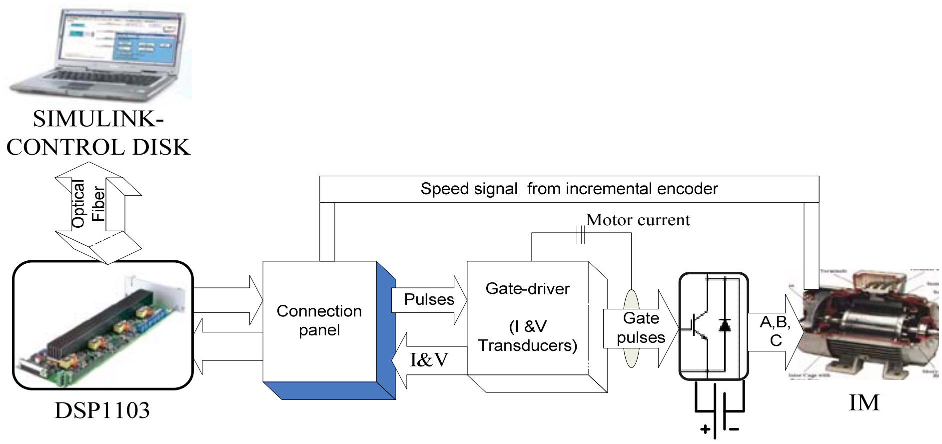

Figure 4. Experimental-setup

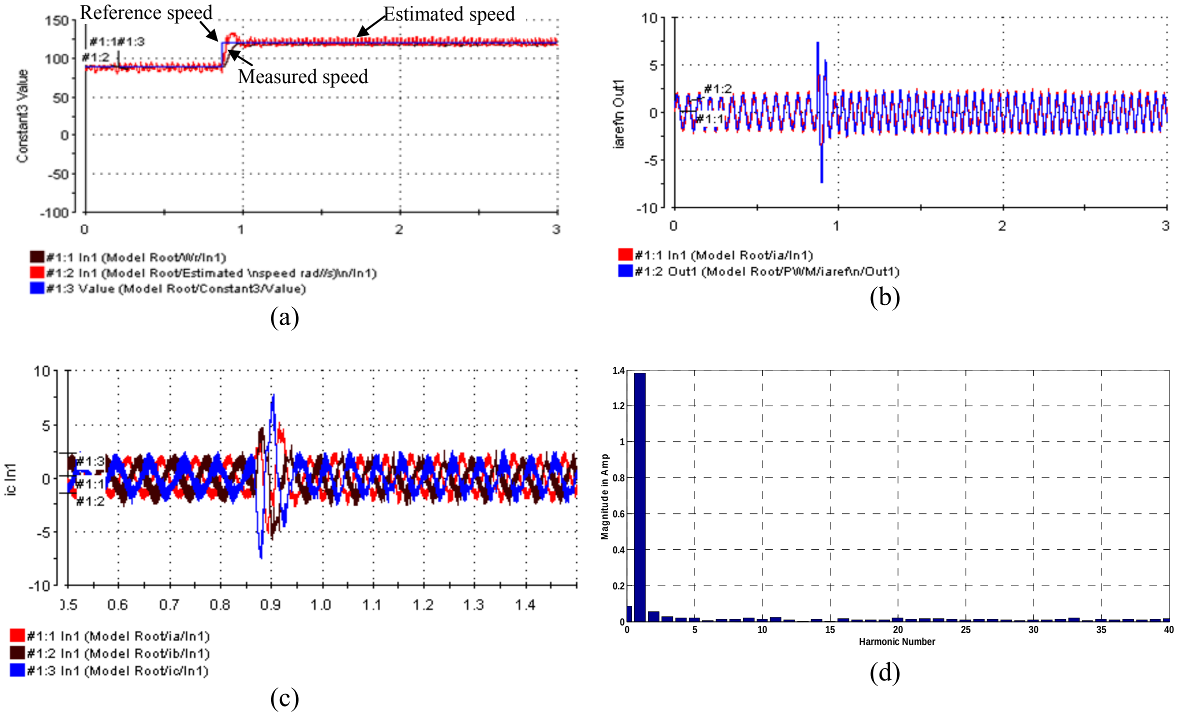

Figure 5. Experimental results of FSTP Drive at no load (a) Motor Speed; (b) Phase current and its reference (c) Three-phase current (d) THD of i_a

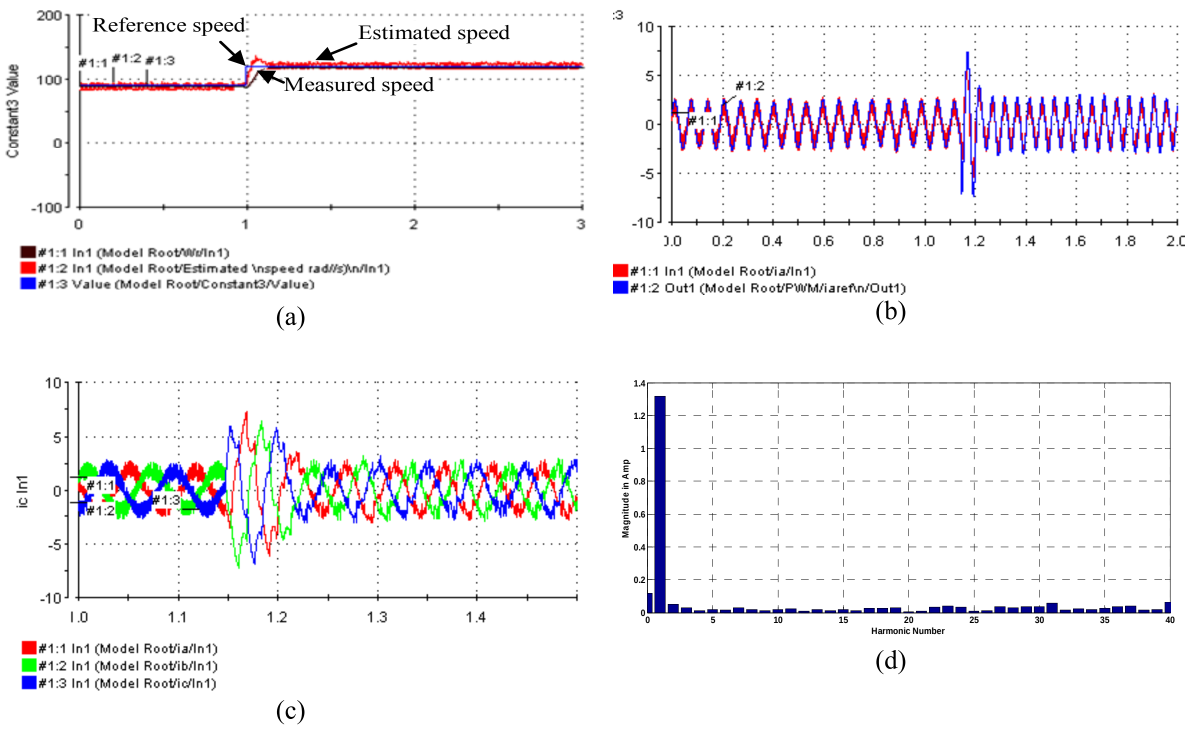

Figure 6. Experimental results of SSTP Drive at no load (a) Motor Speed; (b) Phase current (c) Three-phase current (d) THD of i_a

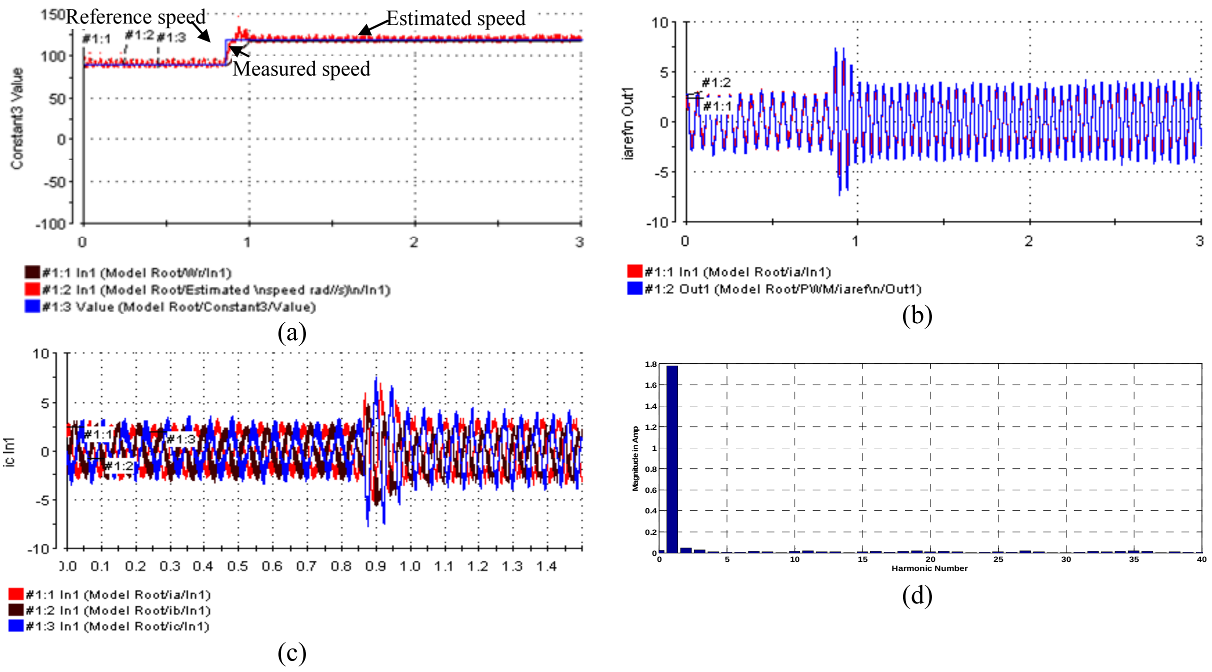

Figure 7. Experimental results of FSTP Drive at full load (a) Speed; (b) Phase current and its reference (c) Three-phase current (d) THD of i_a

In order to provide a fair comparison, the speed responses of the conventional SSTP inverter fed IM drive at identical conditions are shown in Figure 6. It is seen in Figures 6.a that the estimated and measured speed follows the reference speed. Figure 6.b shows the motor phase current whereas figure 6c shows motor three phase current for the step change in speed command. The total harmonic distortion (THD) of i_a is found 24.44% as shown in Figure (6d)

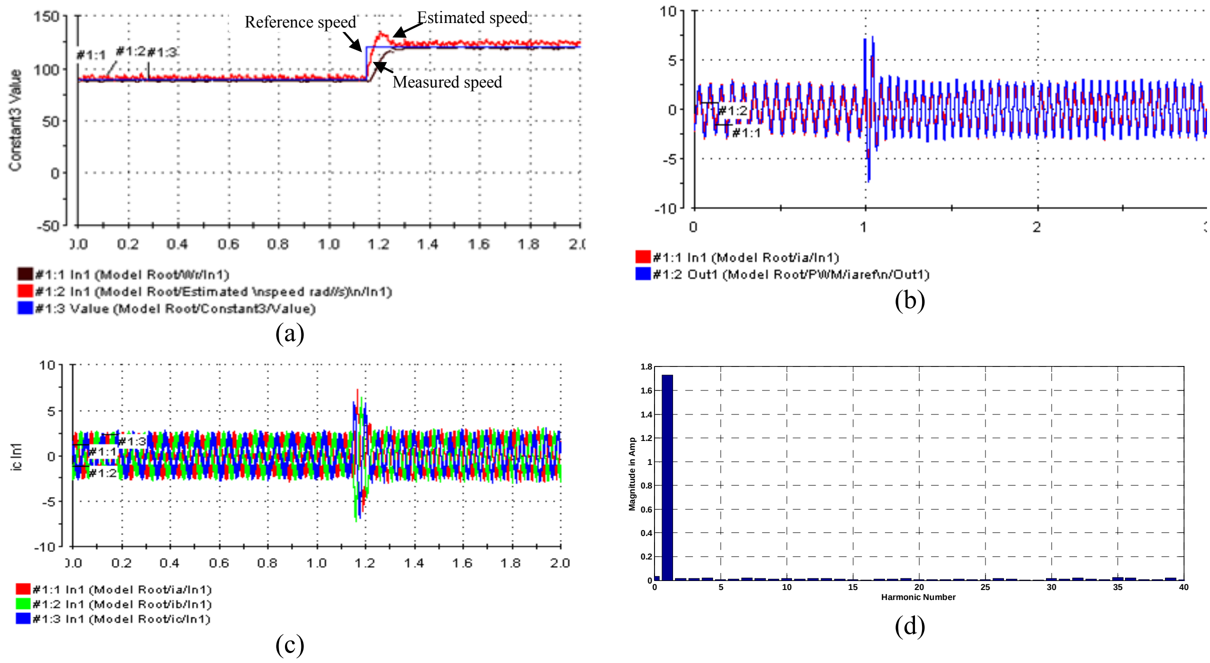

Figure (8) Experimental results of SSTP Drive at full load (a) Speed; (b) Phase current and its reference (c) Three-phase current (d) THD of i_a

Another case to study the drive response. The drive is subjected to step change in the speed reference at full load. Figure 7 shows the drive response when motor fed from FSTP inverter. The motor is running at 90 rad/sec, At t=0.9 second, the speed reference has been changed to 120 rad/sec. it shows that perfect speed tracking with zero steady state error. The response indicates how well the controller succeeds in forcingthe actual rotor speed to follow the desired reference trajectory. With nearly zero steady-state error. Figure 7.b shows motor phase current, whereas figure 7c shows the motor three phase current, it increases with step up of speed reference. The total harmonic distortion (THD) of ia is found 23.5169% as shown in figure 7d. Also, Figures 8 shows the drive response when the motor is fed from SSTP conventional inverter at identical conditions. Figure 8a shows that the estimated and measured speed follows the reference speed with nearly zero steady state error. Figure 8.b shows the motor phase current, whereas figure 8c shows the motor three phase currents for the step change in speed command. The total harmonic distortion (THD) of ia is found 20.2548%. However, after considering all the results, it is seen that the proposed inverter based drive phase currents suffers from slight unbalance in the which cause relatively higher speed vibrations as compared to the conventional 6S3P inverter fed drive. Also, the high switching of motor current makes the estimated speed signal is very noisy in the proposed FSTP drive. The total harmonic distortion of the proposed inverter is slightly increased as compared to conventional inverter. It is found that the performance of the proposed inverter based drive is much closer to that of the conventional inverter and can successfully perform sensorless control.

4. CONCLUSION

A cost-effective FSTP inverter fed IM drive using an MRAS has been implemented. The proposed MRAS-based FSTP inverter fed IM drive system reduces the cost of the inverter, the switching losses and the complexity of the control algorithms as compared with the conventional SSTP inverter based drive. The vector control scheme has been incorporated in the integrated drive system to achieve high performance. The MRAS as a speed estimator verified the robustness of the proposed approach. The performances of the proposed MRAS-based FSTP inverter fed IM drive has been investigated. A comparison of performances for the proposed FSTP inverter fed IM drive with a conventional SSTP inverter fed IM drive has also been made in terms of the speed and total harmonic distortion under identical operating conditions. The proposed FSTP inverter fed IM drive has been found robust and acceptable for low-cost applications such as automotive and home appliance.

REFERENCES

[1] Jin-Su Jang, Byoung-Gun Park, Tae-Sung Kim, Dong Myung Lee, Dong-Seok Hyun. "Sensorless Control of Four-Switch Three-Phase PMSM Drive Using Extended Kalman Filter". *IEEE*. 2008: 1368-1372.

[2] MN Uddin, TS Radwana, and MA Rahman. "Performance analysis of a 4-switch, 3-phase inverter based cost effective IM motor drives". *Electrical and Computer Engineering, Canadian Conference*. 2004: 85–88.

[3] Nasir Uddin, TS Radwan, and MA Rahman. "Performance Analysis of a Cost Effective 4-Switch 3-Phase Inverter Fed IM Drive". *Iranian Journal of Electrical and Computer Engineering*. Summer-Fall. 2006; 5(2).

[4] CB Jacobina, ERC da Silva, AMN Lima, and RLA Ribeiro. "*Vector and scalar control of a four switch three phase inverter*". in Conf. Rec., IEEE-IAS Annu. Meeting. 1995: 2422–2429.

[5] J Holtz. "*Sensorerless Control of Induction Motor Drives*". Proceedings of IEEE. 2002; 90(8): 1359-1394.

[6] CB Jacobina, MB de Rossiter Correa, ERC da Silva, and AMN Lima. "A General PWM Strategy for Four-Switch Three-Phase Inverters". *IEEE Trans. Energy Conversion*. 2006; 21(4): 832-838.

[7] J Klima. "Analytical Investigation of an Induction Motor Fed from Four-Switch VSI with a New Space Vector Modulation Strategy". *IEEE Trans. Power Electron*. 2006; 21(6): 1618-1617.

[8] Nalin Kant Mohanty, Ranganath Muthu, Microcontroller M." Based PWM Controlled Four Switch Three Phase Inverter Fed Induction Motor Drive". *Serbian Journal of Electrical Engineering*. 2010; 7(2): 195-204.

[9] Chul-Woo Park, Woo-Hyen Kwon. "Simple and robust speed sensorless vector control of induction motor using stator current based MRAC". *Electric Power Systems Research*. 2004; 71: 257–266.

[10] dSPdCE. "Digital Signal Proccssingmd Control Engineering". *Manual Guide*. GmhH. Paderhom~ Germany, 2011.

[11] Matlab/Simulink Toolbox User's Guide. The Mathworks Inc., Natick, MA, USA. 1998.

APPENDIX

Machine parameters of the applied induction machine

Rated power	1.1 kw
Rated load torque	7.5 N.m.
No. of poles	4
Stator resistance	7.4826 ohm
Rotor resistance	3.6840 ohm
Rotor leakage inductance	0.0221 H
Stator leakage inductance	0.0221 H
Mutual inductance	0.4114 H
Supply frequency	50 Hz
Motor speed	1500 r.p.m.
Supply voltage	380 volts
Inertia	0.02 kg.m^2

List of Symbols;

$$L_\sigma = L_s - \frac{L_m^2}{L_r} \quad , T_r = \frac{L_r}{R_r} \quad , \sigma = 1 - \frac{L_m^2}{L_s L_r}$$

V_{qse}, V_{dse}	qe-de –axis stator voltage
I_{qse} , I_{dse}	qe-de –axis stator current
λ_{qse} , λ_{dse}	qe-de –axis stator flux linkage
R_s , R_r	stator and rotor resistances
J, B	moment of inertia and viscous friction coefficients
L_s, L_r, L_m	stator, rotor and mutual inductances